All-optical phase modulation for integrated interferometric biosensors

Stefania Dante,[1] Daphné Duval,[1] Borja Sepúlveda,[1] Ana Belen González-Guerrero,[1] José Ramón Sendra,[2] and Laura M. Lechuga[1,*]

[1]*Research Center on Nanoscience and Nanotechnology CIN2 (CSIC) and CIBER-BBN, Campus UAB, 08193 Bellaterra, Barcelona, Spain*

[2]*IUMA, Institute for Applied Microelectronics, University of Las Palmas GC, Las Palmas GC, Spain*

[*]*laura.lechuga@cin2.es*

Abstract: We present the theoretical and the experimental implementation of an all-optical phase modulation system in integrated Mach-Zehnder Interferometers to solve the drawbacks related to the periodic nature of the interferometric signal. Sensor phase is tuned by modulating the emission wavelength of low-cost commercial laser diodes by changing their output power. FFT deconvolution of the signal allows for direct phase readout, immune to sensitivity variations and to light intensity fluctuations. This simple phase modulation scheme increases the signal-to-noise ratio of the measurements in one order of magnitude, rendering in a sensor with a detection limit of $1.9 \cdot 10^{-7}$ RIU. The viability of the all-optical modulation approach is demonstrated with an immunoassay detection as a biosensing proof of concept.

OCIS codes: (120.3180) Interferometry; (120.5060) Phase modulation; (130.3120) Integrated optics devices; (280.1415) Biological sensing and sensors; (280.4788) Optical sensing and sensors.

References and links

1. X. Fan, I. M. White, S. I. Shopova, H. Zhu, J. D. Suter, and Y. J. Sun, "Sensitive optical biosensors for unlabeled targets: a review," Anal. Chim. Acta **620**(1-2), 8–26 (2008).
2. M. C. Estevez, M. Álvarez, and L. M. Lechuga, "Integrated Optical devices for lab-on-a-chip biosensing applications," Laser Photon. Rev. DOI: 10.1002/lpor.201100025 (2011).
3. A. Ymeti, J. S. Kanger, R. Wijn, P. V. Lambeck, and J. Greve, "Development of a multichannel integrated interferometer immunosensor," Sens. Actuators B Chem. **83**(1-3), 1–7 (2002).
4. K. Schmitt, B. Schirmer, C. Hoffmann, A. Brandenburg, and P. Meyrueis, "Interferometric biosensor based on planar optical waveguide sensor chips for label-free detection of surface bound bioreactions," Biosens. Bioelectron. **22**(11), 2591–2597 (2007).
5. G. Heideman and P. V. Lambeck, "Remote opto-chemical sensing with extreme sensitivity: design, fabrication and performance of a pigtailed integrated optical phase-modulated Mach–Zehnder interferometer system," Sens. Actuators B Chem. **61**(1-3), 100–127 (1999).
6. B. Sepúlveda, J. Sánchez del Río, M. Moreno, F. J. Blanco, K. Mayora, C. Domínguez, and L. M. Lechuga, "Optical biosensor micro-systems based on the integration of highly sensitive Mach-Zehnder interferometer devices," J. Opt. A, Pure Appl. Opt. **8**(7), S561–S566 (2006).
7. B. H. Schneider, E. L. Dickinson, M. D. Vach, J. V. Hoijer, and L. V. Howard, "Optical chip immunoassay for hCG in human whole blood," Biosens. Bioelectron. **15**(11-12), 597–604 (2000).
8. D. J. Bornhop, J. C. Latham, A. Kussrow, D. A. Markov, R. D. Jones, and H. S. Sørensen, "Free-solution, label-free molecular interactions studied by back-scattering interferometry," Science **317**(5845), 1732–1736 (2007).
9. K. E. Zinoviev, A. B. González-Guerrero, C. Domínguez, and L. M. Lechuga, "Integrated Bimodal Waveguide Interferometric Biosensor for Label-free Analysis," J. Lightwave Technol. **29**(13), 1926–1930 (2011).
10. B. Sepúlveda, G. Armelles, and L. M. Lechuga, "Magneto-optical phase modulation in integrated Mach–Zehnder interferometric sensors," Sens. Actuators A Phys. **134**(2), 339–347 (2007).
11. K. Preston, S. Manipatruni, A. Gondarenko, C. B. Poitras, and M. Lipson, "Deposited silicon high-speed integrated electro-optic modulator," Opt. Express **17**(7), 5118–5124 (2009).
12. M. B. Dühring and O. Sigmund, "Improving the acousto-optical interaction in a Mach-Zehnder interferometer," J. Appl. Phys. **105**(8), 083529 (2009).

#159373 - $15.00 USD Received 5 Dec 2011; revised 3 Feb 2012; accepted 6 Feb 2012; published 14 Mar 2012

13. P. Dumais, C. L. Callender, J. P. Noad, and C. J. Ledderhof, "Integrated optical sensor using a liquid-core waveguide in a Mach-Zehnder interferometer," Opt. Express **16**(22), 18164–18172 (2008).
14. V. Passaro, F. Magno, and A. Tsarev, "Investigation of thermo-optic effect and multi-reflector tunable filter/multiplexer in SOI waveguides," Opt. Express **13**(9), 3429–3437 (2005).
15. A. Dér, S. Valkai, A. Mathesz, I. Andó, E. K. Wolff, and P. Ormos, "Protein-based all-optical sensor device," Sens. Actuators B Chem. **151**(1), 26–29 (2010).
16. A. Dandridge and A. B. Tveten, "Phase compensation in interferometric fiber-optic sensors," Opt. Lett. **7**(6), 279–281 (1982).
17. U. Minoni, E. Sardini, E. Gelmini, F. Docchio, and D. Marioli, "A high-frequency sinusoidal phase-modulation interferometer using an electro-optic modulator: Development and evaluation," Rev. Sci. Instrum. **62**(11), 2579–2583 (1991).
18. D. Guo, M. Wang, and S. Tan, "Self-mixing interferometer based on sinusoidal phase modulating technique," Opt. Express **13**(5), 1537–1543 (2005).
19. F. Prieto, B. Sepúlveda, A. Calle, A. Llobera, C. Domínguez, A. Abad, A. Montoya, and L. M. Lechuga, "An integrated optical interferometric nanodevice based on silicon technology for biosensor applications," Nanotechnology **14**(8), 907–912 (2003).
20. K. Zinoviev, L. G. Carrascosa, J. Sánchez del Río, B. Sepúlveda, C. Domínguez, and L. M. Lechuga, "Silicon Photonic Biosensors for Lab-on-a-Chip Applications," Adv. Opt. Technol. **2008**, 383927 (2008).
21. T. Gao and L. J. Rothberg, "Label-free sensing of binding to microarrays using Brewster angle straddle interferometry," Anal. Chem. **79**(20), 7589–7595 (2007).
22. Y. Chen, P. Xu, M. Liu, and X. Li, "Bio/chemical detection in liquid with self-sensing Pr-Oxi-Lever (piezo-resistive SiO2 cantilever) sensors," Microelectron. Eng. **87**(12), 2468–2474 (2010).

1. Introduction

Integrated optical sensors have emerged during the last decades as one of the most promising candidates for Lab-on-Chip implementation. These sensors have the required properties of high sensitivity, miniaturized size, multiplexed format for array implementation and CMOS compatible fabrication processes for such application. Among the different integrated optical transducers, the interferometric sensors are one of the most sensitive configurations, with detection limits in the range 10^{-6}-10^{-8} RIU [1,2]. Several successful implementations have been published as Young [3,4], Mach-Zehnder [5,6], Hartman [7], Back-Scattering [8] or more recently Bimodal waveguide [9] interferometers.

But despite their high sensitivity, their label-free and real-time scheme of detection and the innate advantages offered by an interferometric configuration, there is still no successful commercial biosensor based on Mach-Zehnder (MZI) principle. One of the main reasons is related to the complex read-out of the interferometric response and to its high dependence on variables as the input source fluctuations or temperature variations, which can give false positive signals.

We present here a new phase modulation system based on an all-optical approach able to solve the limitations of the interferometric detections. The required phase change is introduced by tuning the input wavelength of a commercial Fabry-Perot laser diode and taking advantage of the asymmetric interferometric configuration imposed by the sensing area in one of the arms of the interferometer. In section 2 we first review the working principle of the standard MZI biosensor, describing the problems arising from its periodic output nature and the state-of-the-art in phase modulation techniques to control its output. In section 3 the theoretical analysis of the all-optical wavelength modulation working principle is provided, while in section 4 the experimental verification of the method is shown. Finally, in section 5, we present the calibration curve of the modulated sensor to refractive index changes, the comparison with a standard MZI detection scheme (without modulation) and a biosensing proof of concept with the detection of the human Growth Hormone (hGH) by an immunoassay.

2. Standard Mach-Zehnder Interferometer

In an integrated MZI, the light traveling in a rib waveguide is split into two arms, the sensing and the reference arms, by a Y-junction. The two beams are recombined again, after a certain

#159373 - $15.00 USD Received 5 Dec 2011; revised 3 Feb 2012; accepted 6 Feb 2012; published 14 Mar 2012

distance, in a second Y-junction, producing their interference. A scheme of the sensor is shown in Fig. 1.

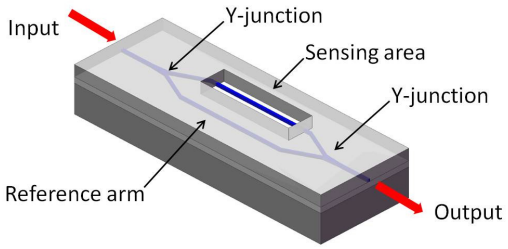

Fig. 1. MZI scheme. A rib waveguide is split into two arms (reference and sensing) which recombine again into a single output waveguide.

For biosensing applications, the protective cladding is removed from a portion of the sensing arm, the so-called sensing area, where the evanescent field of the propagating mode can probe the external medium, thus providing an asymmetric interferometric configuration. A change of the refractive index in the sensing area, as the one generated by biochemical interactions, will change the effective refractive index of the guided mode, inducing a phase difference between the light beams travelling in both arms. Such phase difference will result in an intensity variation at the output of the device that can be expressed as:

$$I_T = I_S + I_R + 2\sqrt{I_S I_R}\cos\left[\Delta\varphi_S(t)\right] \quad (1)$$

where I_S and I_R are the intensities of the light in the sensor and reference arms, respectively. The term $\Delta\varphi_S$ is the phase difference between the light beams travelling in both arms, and is given by:

$$\Delta\varphi_S(t) = 2\pi\frac{L}{\lambda}\left(N_S(t) - N_R\right) \quad (2)$$

where N_S and N_R are the effective refractive indexes of the guided modes in the sensor and reference arms, respectively, λ is the wavelength of light and L is the length of the sensing area. As it can be deduced from Eq. (1), the output intensity of the interferometric device is periodic with respect to the phase changes induced in the sensing area.

Because of the periodic nature of the output signal, the MZI response can give rise to wrong or ambiguous interpretations. There are three main issues related to this type of signal: ambiguity, sensitivity fading and intensity fluctuations leading to false positives [5,10]. Signal ambiguity prevents the discrimination between two values differing of an integer multiple of 2π and impedes the prediction of the phase evolution direction when the phase difference between the two arms is an integer multiple of π. At the same time, sensitivity suffers the same periodicity of phase evolution, i.e. is not constant but maximum at quadrature point and minimum at curve extremes. Furthermore, input light or temperature fluctuations can give rise to false positive signals which can constitute a serious issue for having reliable sensor devices and must be carefully handled.

All these drawbacks can be solved by tuning the phase difference between the arms of the interferometer device. Various solutions have been suggested in the last years, the most common are based on electro-optical [5,11], acousto-optical [12], thermo-optical [13,14] or magneto-optical [10] working principles. A different approach, recently described in [15], consists in depositing a light-sensitive adlayer on the reference arm and controlling its refractive index upon light intensity variations. The disadvantages of all the above techniques rely in the need of complex fabrication processes, often requiring not standard CMOS compatible materials, in the need of electrodes and electrical connections, conflicting with

#159373 - $15.00 USD Received 5 Dec 2011; revised 3 Feb 2012; accepted 6 Feb 2012; published 14 Mar 2012

microfluidics, and in the complex electronic equipment required for the read-out, seriously hindering the miniaturization of the interferometric devices for Lab-on-Chip implementation.

3. Overview of the technique

3.1 All-optical phase modulation principle

In contrast to the above described technologically challenging phase modulation methods, we propose a straightforward and cost effective approach based on the power-dependent wavelength variations of commercial Fabry-Perot laser diodes [16] and on the asymmetry of the MZI sensors. This method permits to introduce a periodical phase change between the arms of the interferometer by applying a periodical driving current to the laser diode. The output signal is analyzed with Fourier transform.

If we consider a sinusoidal phase modulation function, $f(\nu_M) = \mu_M \sin(\omega_M t)$, and we assume that the period of the modulation is much shorter than the response time of the biosensing interactions (which are typically in the order of seconds or minutes), the standard Mach-Zehnder output given by Eq. (1) is transformed into:

$$I_T = I_S + I_R + 2\sqrt{I_S I_R}\cos\left[\mu_M \sin(\omega_M t) + \Delta\varphi_S(t)\right] \tag{3}$$

Equation (3) can be expanded in a Fourier series [17,18], resulting in:

$$I_T = I_S + I_R + 2\sqrt{I_S I_R}\begin{Bmatrix}\cos\left(\Delta\varphi_S(t)\right)\left[J_0(\mu_M) + 2\sum_{n=1}^{\infty} J_{2n}(\mu_M)\cos\left(2n\omega_M t\right)\right] + \\ \sin\left(\Delta\varphi_S(t)\right)\left[2\sum_{n=0}^{\infty} J_{2n+1}(\mu_M)\sin\left((2n+1)\omega_M t\right)\right]\end{Bmatrix} \tag{4}$$

where J_n is the Bessel function of order n. Therefore, the DC term and the first three harmonics are given by:

$$\begin{cases} I_{DC} = I_S + I_R + 2\sqrt{I_S I_R}\cos\left(\Delta\varphi_S(t)\right)J_0(\mu_M) \\ I_{1\omega} = 4\sqrt{I_S I_R}\sin\left(\Delta\varphi_S(t)\right)J_1(\mu_M) \\ I_{2\omega} = 4\sqrt{I_S I_R}\cos\left(\Delta\varphi_S(t)\right)J_2(\mu_M) \\ I_{3\omega} = 4\sqrt{I_S I_R}\sin\left(\Delta\varphi_S(t)\right)J_3(\mu_M) \end{cases} \tag{5}$$

According to these expressions, phase information can in principle be extracted by considering the ratio of any pair of consecutive harmonics. The ratio of the generic pair of harmonics with indexes $2n\omega$ and $(2n+1)\omega$ is given by:

$$\frac{I_{(2n+1)\omega}}{I_{2n\omega}} = \frac{\sin\left(\Delta\varphi_S(t)\right)J_{(2n+1)}(\mu_M)}{\cos\left(\Delta\varphi_S(t)\right)J_{2n}(\mu_M)} \tag{6}$$

Thus, by choosing a modulation amplitude μ_M that satisfies:

$$J_{2n}(\mu_M) = J_{(2n+1)}(\mu_M) \tag{7}$$

$\Delta\varphi$ can be directly extracted from:

$$\Delta\varphi_S(t) = \arctan\left(\frac{I_{(2n+1)\omega}}{I_{2n\omega}}\right) \tag{8}$$

According to Bessel functions' theory, it is possible to find a value of μ_M satisfying Eq. (7) for each couple of consecutive harmonics. This value is 0.84π in the case $J_1(\mu_M) = J_2(\mu_M)$, 1.2π for $J_2(\mu_M) = J_3(\mu_M)$ and 1.55π for $J_3(\mu_M) = J_4(\mu_M)$.

#159373 - $15.00 USD Received 5 Dec 2011; revised 3 Feb 2012; accepted 6 Feb 2012; published 14 Mar 2012

During this study, harmonics $I_{2\omega}$ and $I_{3\omega}$ are employed to extract the phase information since in practice they demonstrated to be more stable and reliable than the pair $I_{1\omega}$-$I_{2\omega}$ due to the different laser behavior in response to the applied modulation amplitude.

In this modulation scheme the phase change is not deduced anymore from the variations of the intensity interference pattern but is directly extracted from the periodically modulated output, as shown by Eq. (8). Therefore, this phase modulation approach overcomes the three problems derived from the periodicity of the output signal described in section 2.

3.2 Numerical study of the wavelength modulation

According to Eq. (2) and to the fact that the effective refractive index depends on the propagating light wavelength, a phase change between the arms of the interferometer can be induced by a change in the laser wavelength. The introduction of a small change (few nm) in the wavelength of the guided light will produce a variation of the phase difference given by:

$$\delta(\Delta\varphi_S) = \frac{2\pi}{\lambda}\left[-\frac{1}{\lambda}(N_S - N_R) + \frac{\partial(N_S - N_R)}{\partial\lambda}\right]L\delta\lambda \qquad (9)$$

where the second term in the right side of Eq. (9) is much smaller than the first term and can be neglected.

The wavelength modulation amplitude ($\delta\lambda$) necessary to induce a given phase change between the two interferometer arms can be numerically evaluated as a function of the core thickness of the MZI devices, using the simplified form of Eq. (9). For this purpose, we consider a waveguide structure similar to the one described in [6,19]. In this structure, a Si_3N_4 core is embedded between two SiO_2 cladding layers (2 μm thickness each), except in the sensing area, where the top cladding is the environment (water). In Fig. 2 we represent the results of this numerical simulation in the case of a phase change of 2π, for TE and TM polarizations, assuming L = 15 mm, λ_0 = 660 nm, a rib of 1 nm (height) × 4 μm (width) as in our experimental devices and water as the external medium in the sensing area (n = 1.33).

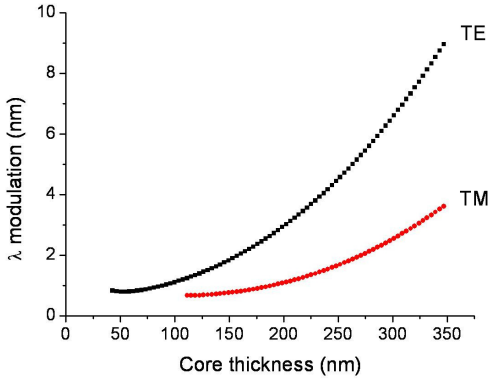

Fig. 2. Wavelength modulation amplitude needed to achieve a 2π phase modulation, as a function of core thickness and the light polarization.

According to the results shown in Fig. 2, for a core thickness of 200 nm the required $\Delta\lambda$ inducing a 2π phase change is 1.1 nm in the case of TM polarization, enabling the use of common Fabry-Perot laser diodes. Even if the employment of laser diodes with respect to gas lasers is generally discouraged due to their worst performances in terms of temperature stability and signal-to-noise ratio (SNR) in standard conditions [5], the advantages coming from a direct phase read-out implementation, their lower cost, smaller size and facility of hybrid integration justify their use.

#159373 - $15.00 USD Received 5 Dec 2011; revised 3 Feb 2012; accepted 6 Feb 2012; published 14 Mar 2012

4. Implementation of the wavelength modulation system

4.1Laser diode characterization

The output light of a commercial laser diode (ML101J27, Mitsubishi: nominal wavelength λ_0 = 660 nm) is focused at the input of a MZI device. The light intensity is periodically modulated with a sinusoidal profile by a voltage input supplied through an acquisition card, controlled by a dedicated Labview software. Laser optical cavity temperature is kept constant by a temperature controller (ITC510, Thorlabs), whereas precision micro-position stages allow the alignment of the optical components (Nanomax-TS, Thorlabs).

We first study the wavelength dependence of the laser diode. Figure 3(a) shows the emission spectra of the laser diode source in static conditions and at T = 25°C at different driving currents. From these experimental data, a linear relationship can be found between driving current and peak wavelength: $\lambda(I_{LD}) = 0.039 \cdot I_{LD} + 655.813nm$, as represented in Fig. 3(b).

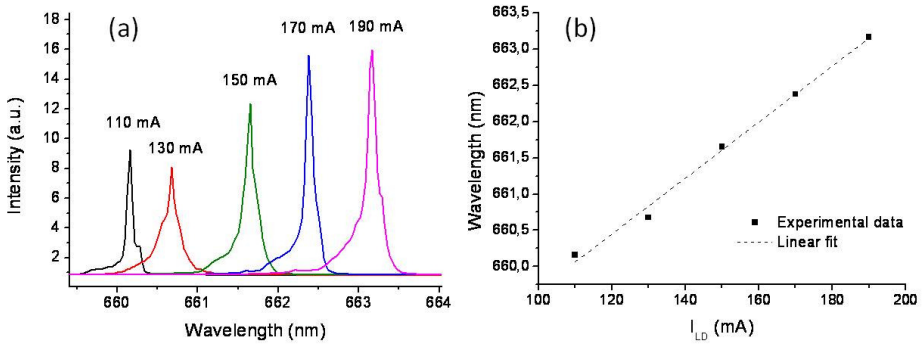

Fig. 3. (a) Emission spectra of the laser diode, acquired in static conditions at T = 25°C at different driving currents; the maximum wavelength shift approaches 3 nm. (b) Plot of the emission wavelength versus driving current.

4.2 Verification of the wavelength modulation principle

In order to proof the wavelength modulation principle we keep constant the refractive index on the sensing area by flowing milli-Q grade water (n = 1.3328) while we slowly vary the input laser wavelength by tuning the laser driving current (I_{LD}).

Figure 4 shows the results for a MZI device with silicon nitride core thickness of 200 nm, characterized in TM polarization. Output intensity shows periodical variations as predicted from Eqs. (1) and (2). By relating the period of these oscillations to the laser spectra it is possible to obtain the wavelength shift necessary to induce a 2π phase shift. In this case, the wavelength shift is evaluated as 1.2 nm, which is in good agreement with the theoretical prediction of 1.1 nm (Fig. 2).

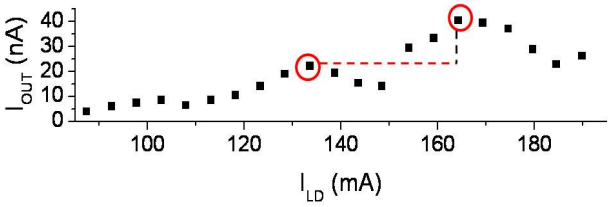

Fig. 4. Evolution of MZI output versus input current (wavelength) in the case of TM input light for a MZI device with 200 nm core.

#159373 - $15.00 USD Received 5 Dec 2011; revised 3 Feb 2012; accepted 6 Feb 2012; published 14 Mar 2012

4.3 Data processing

Accordingly to the mathematical development presented in section 3.1, the parameters for modulating the input laser beam are the DC intensity working point, the modulation amplitude and the modulation frequency. All the data operations are done in real-time using Labview software.

Data processing is illustrated in the following with the example of the detection of an index change $\Delta n = 5 \cdot 10^{-4}$ RIU, obtained by flowing a solution of HCl 0.05M with milli-Q water as running buffer on the device sensing area.

The interferometer output (I_T) is normalized by a reference signal (I_{REF}, see Fig. 5(a)) to eliminate unwanted amplitude modulation effects. This reference is extracted from the optical path using a beam splitter placed before the interferometer input. Fast Fourier Transform (FFT), shown in Fig. 5(b), is then evaluated on the quotient $I_N(t) = I_T/I_{REF}$. Figure 5(c) shows the intensities of second and third harmonics, extracted from real and imaginary parts of the FFT, respectively $\mathrm{Re}\{I_{2\omega}\}$ and $\mathrm{Im}\{I_{3\omega}\}$, in the case of detection of this index change. To set the working point, the condition on Bessel functions stated by Eq. (7) must be fulfilled. In practice, to compensate the non-ideal laser diode behavior and the minor variations of the device due to fabrication, modulation parameters have to be slightly varied around the theoretical value (1.2π) till the amplitudes of the two considered harmonics are equal.

As stated by Eq. (8), phase information can be directly extracted from the inverse tangent evaluated on the ratio of two consecutive harmonics, resulting in a signal oscillating in the range $\pm \pi$ (see Fig. 5(d)). Due to the linearity of the inverse tangent and to the abrupt jumps described in correspondence of $\pm \pi$ values, it can be easily unwrapped in real-time to get a smoother and continuous cumulative response (Fig. 5(e)), unaffected by ambiguities.

Moreover, as the phase change information is directly provided and not deduced from the sinusoidal output of the standard MZI device, evaluation is not influenced anymore by the visibility factor (fringes amplitude) and it is immune to the problems related to the periodic nature of interferometric output. A theoretically infinite dynamic range is obtained, since unwrapped phase evolution is no more constrained.

#159373 - $15.00 USD Received 5 Dec 2011; revised 3 Feb 2012; accepted 6 Feb 2012; published 14 Mar 2012

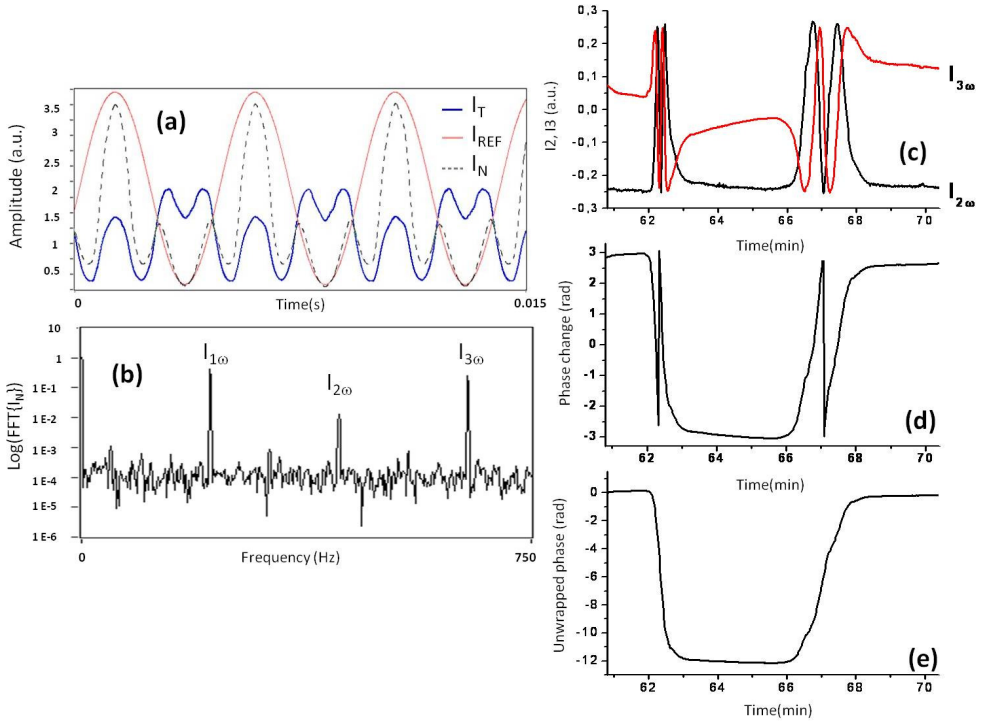

Fig. 5. (color online) Steps of data processing, starting from signals acquisition and ending in direct and real-time data output. The steps are illustrated in the case of the detection of a refractive index change of $\Delta n = 5 \cdot 10^{-4}$ RIU. (a) Screenshot of acquired signals I_T and I_{REF} and their ratio I_N, (b) FFT evaluated on I_N, (c) $I_{2\omega}$ and $I_{3\omega}$ harmonics evolution during the index change, (d) phase signal and (e) unwrapped phase signal.

5. Results and discussion

5.1 Homogeneous sensing

In order to check the suitability of the technique for evaluating the sensitivity of the MZI device, a calibration curve measuring the phase changes induced by refractive index variations was carried out. PDMS channels embedded in a PMMA housing have been employed to supply the fluids to the sensing area. A peristaltic pump (Minipuls 3, Gilson) is used to maintain a constant flow regime. Different concentrations of HCl (0.2M, 0.1M, 0.05 M and 0.025 M) have been injected with running water (milli-Q grade) as buffer. Previously to injection, the refractive index of the solutions has been measured with an ABBE Refractometer (Optic Ivymen System, Spain). Table 1 reports the absolute refractive indexes of the HCl solutions used for calibration and the index changes induced in the MZI sensing area considering milli-Q water (n = 1.3328) as buffer.

Table 1. Refractive Indexes of the Set of HCl Solutions Used For Calibration

Solution	n	Δn
HCl 0.2 M	1.3345	$1.7 \cdot 10^{-3}$
HCl 0.1 M	1.3337	$9 \cdot 10^{-4}$
HCl 0.05 M	1.3333	$5 \cdot 10^{-4}$
HCl 0.025 M	1.3331	$3 \cdot 10^{-4}$

Figure 6(a) shows the real-time phase evolution of the wavelength modulated MZI during the injection of the different concentrations of HCl, with milli-Q grade water as a running buffer. Phase starts from a constant level (corresponding to water) and varies when HCl

#159373 - $15.00 USD Received 5 Dec 2011; revised 3 Feb 2012; accepted 6 Feb 2012; published 14 Mar 2012

reaches the sensing area ("HCl ON" in Fig. 6(a)); then stabilizes and returns to the starting level when milli-Q water arrives again to the sensor area ("OFF"). The parameters employed for the modulation were a DC current of 138 mA, a modulation amplitude of 36 mA and a frequency of 215 Hz. All measurements have been done in TM polarization.

As a result, Fig. 6(b) shows the calibration curve obtained after the evaluation of the phase changes corresponding to each of the refractive index changes reported in Table 1.

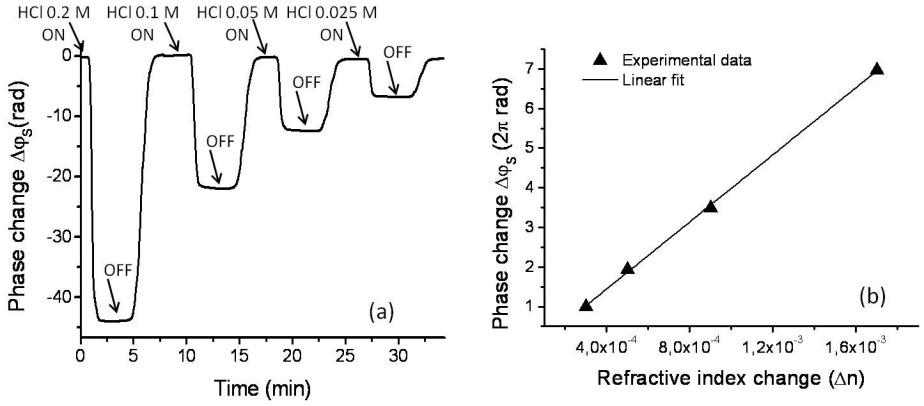

Fig. 6. (a) Real-time evolution of the phase change on a wavelength modulated MZI, subjected to different HCl injections. (b) Calibration curve. Detection of $\Delta n = 3 \cdot 10^{-4}$ giving $\Delta\varphi = 0.99 \cdot 2\pi$ rad, $\Delta n = 5 \cdot 10^{-4}$ giving $\Delta\varphi = 1.94 \cdot 2\pi$ rad, $\Delta n = 9 \cdot 10^{-4}$ giving $\Delta\varphi = 3.5 \cdot 12\pi$ rad and $\Delta n = 1.7 \cdot 10^{-3}$, giving $\Delta\varphi = 6.97 \cdot 2\pi$ rad.

The sensitivity has been evaluated as the slope (k) of the curve $\Delta\varphi$ versus Δn. A linear fit gives $k = 4240 \cdot 2\pi$ rad/RIU, with $R^2 = 0.999$. The detection limit of the sensor can be estimated by considering that the lowest detectable phase, $\Delta\varphi_{S,min}$, is equal to three times the standard deviation (σ) of the system. Since $\Delta n_{\min} = \dfrac{\Delta\varphi_{S,\min}}{k}$ and $\sigma = 0.0017$ rad, we obtain a theoretical detection limit of $1.9 \cdot 10^{-7}$ RIU.

5.2 Sensor performance and advantages over standard MZI

In order to compare the wavelength modulation approach with the standard configuration, the same chip has been analyzed with the same laser diode without modulation (monochromatic light) and with the wavelength modulation technique, both for TM polarization. The measurements have been compared in terms of SNR, after performing a linear fit on the same population of experimental data along a constant part of the two curves. According to the definition SNR = x/σ, the signal value x has been considered equal to twice the fringe amplitude in the case of a standard detection, which corresponds to 2π in the case of the wavelength modulated MZI.

Figure 7 shows the detection of a bulk index change $\Delta n = 5 \cdot 10^{-4}$ RIU on a chip of 250 nm core thickness, in the case of the standard interferometric pattern (Fig. 7(a)) and in the case of the unwrapped phase obtained with wavelength modulation (Fig. 7(b)).

#159373 - $15.00 USD Received 5 Dec 2011; revised 3 Feb 2012; accepted 6 Feb 2012; published 14 Mar 2012

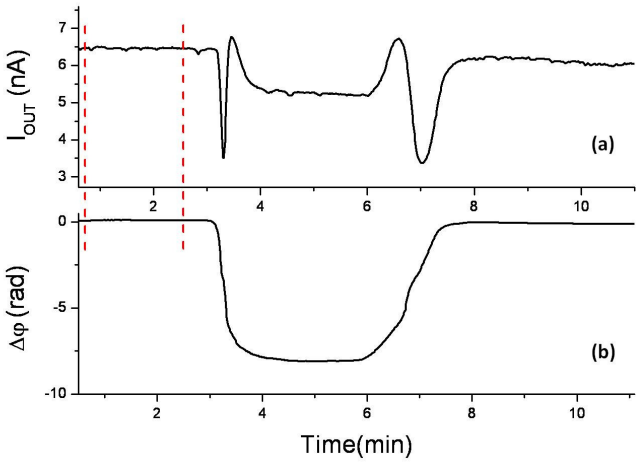

Fig. 7. Comparison of sensor response in the case of (a) standard interferometric pattern, with monochromatic light excitation and (b) unwrapped phase with λ-modulated input, in the case of detection of a bulk index change $\Delta n = 5 \cdot 10^{-4}$ RIU. Standard deviation has been evaluated by a linear fit over the constant part of the two curves (regions in evidence).

We obtained a value of $\sigma = 2.19 \cdot 10^{-5}$ μA in the case of standard MZI and $\sigma = 2.34 \cdot 10^{-3}$ rad in the case of λ-modulated MZI, corresponding to SNR = 299 and 2685, respectively. The employment of the wavelength modulation results in a 9 times fold improvement in the system SNR. Moreover, the limit of detection (LOD) obtained with the wavelength modulation is comparable to the one obtained in previous studies using a He-Ne laser [20].

In addition to the improved SNR, false read-out responses due to input intensity variations, related to laser instabilities or mechanical misalignments, are also eliminated with this detection scheme. It is important to underline that these results have been achieved using a compact, small and easily integrated laser diode instead of a bulky He-Ne one. This fact strongly supports the adoption of the wavelength modulation approach for the achievement of a sensitive and real-time Lab-on-Chip device with an interferometric biosensor.

5.3 Biosensing evaluation

In order to fully demonstrate the viability of our all-optical modulated MZI device for biosensing applications, we have evaluated the immunoreaction of the pair hGH/anti-hGH (human Growth Hormone, Sigma) using the modulated MZI sensor. hGH was previously immobilized on the sensor surface following standard silanization protocols and the specific antibody (mAb-hGH) was flowed through the sensor area for detection.

A solution 50 μg/ml of hGH was covalently immobilized on the sensing area of the MZI after silanization of the silicon nitride surface with Carboxyethylsilanetriol, sodium salt (CTES) as silane agent. Carboxylic groups were activated by N-(3-dimethylaminopropyl)-N'-ethylcarbodiimide (EDC)/ N-Hydroxysuccinimide (NHS) incubation [21,22].

Two concentrations of specific antibody were injected in a volume of 250 μl and the receptor surface was regenerated by flowing a solution of HCl 10 mM between the two immunoreactions. Figure 8 shows the phase response for both antibody concentrations (1 μg/ml and 5 μg/ml).

#159373 - $15.00 USD Received 5 Dec 2011; revised 3 Feb 2012; accepted 6 Feb 2012; published 14 Mar 2012

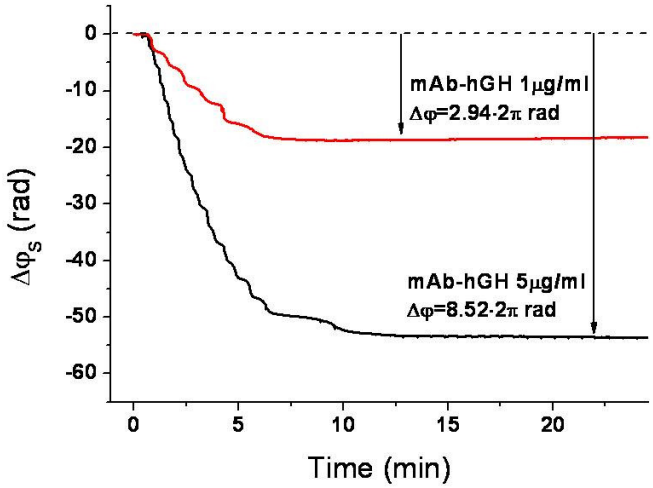

Fig. 8. Real-time phase change induced by the immunoreaction of mAb-hGH of 5 μg/ml mAb-hGH, inducing $\Delta\varphi = 8.52 \cdot 2\pi$ rad (black line) and 1 μg/ml mAb-hGH, giving $\Delta\varphi = 2.94 \cdot 2\pi$ rad (red line).

These results clearly validate the use of the wavelength modulated MZI as a direct biosensor device. The direct phase read-out extremely simplifies data analysis, making it a perfect candidate for portable sensing platforms.

6. Conclusion

In this paper we have proposed an innovative phase modulation system able to solve the problems arising from the periodic nature of the MZI sensor output. We have demonstrated a simple, low-cost and effective modulation technique that takes advantages of a well known drawback of semiconductor laser diodes: by controlling the laser driving current, it is possible to create a periodical wavelength variation that induces a phase modulation along the asymmetric interferometer arms. With this approach, no additional fabrication processes neither electrical pads are necessary.

The validity of this approach has been demonstrated with the calibration of the device to refractive index changes, resulting in a detection limit of $1.9 \cdot 10^{-7}$ RIU. The employment of the wavelength modulation gives a 9 times fold improvement in the system SNR compared to standard detection scheme (without modulation). The LOD demonstrated in this work is comparable to the one obtained using a He-Ne laser. The suitability for biosensing applications has been demonstrated by an immunoreaction detection.

The real-time and direct phase read-out proposed here opens outstanding horizons for the commercialization and integration into Lab-on-Chip platforms of the wavelength modulated MZI. The wavelength modulation principle has been investigated and demonstrated in the case of the integrated MZI but can be extended to other interferometric configurations.

Acknowledgments

This work was partially developed using the micro and nano fabrication capabilities of the ICTS/clean room from the IMB-CNM (CSIC), under project NGG249 and has been sponsored by Fundación M. Botin. S. Dante acknowledges the "Programa de Formación de Profesorado Universitario (FPU)" of the "Ministerio de Educación" of Spain and B. Sepulveda acknowledges the "Ramón y Cajal" program from "Ministerio de Ciencia e Innovación" of Spain for financial support.

#159373 - $15.00 USD Received 5 Dec 2011; revised 3 Feb 2012; accepted 6 Feb 2012; published 14 Mar 2012